THE EFFECT OF MICROSTRUCTURE ON MECHANICAL PROPERTIES OF HVOF SPRAYED WC-COCR COMPOSITE COATINGS

T. SUHONEN[1,*], T. VARIS[1], E. TURUNEN[1], X. LIU[2], Y. GE[2], O. SÖDERBERG[2], S-P. HANNULA[2]

[1] *VTT Technical Research Centre of Finland, Advanced Materials, P.O.Box 1000, 02044 VTT, Finland*
[2] *Helsinki University of Technology, Department of Materials Science P.O.Box 6200, 02015 TKK, Finland*
[*] *Corresponding author. Tel.: +358 40 5012163; fax: +358 20 7227069; e-mail: tomi.suhonen@vtt.fi*

ABSTRACT

This study aims for deeper understanding of the composition and phase changes occurring during HVOF spraying of the powder to WC-CoCr coatings. Also, the effect of lamellar microstructure on the mechanical properties is studied. Compositional and microstructural features are studied by means of X-ray diffraction, XRF, FE-SEM and TEM (EDX, EELS). Mechanical properties are mainly studied by different instrumented indentation and nanoindentation techniques. The use of two new fracture parameters, complementing the fracture toughness value of the coating, are proposed and examined. Higher load range indentations are used to measure cross-sectional and surface hardness, elastic modulus and fracture toughness of the coatings. Mechanical properties of individual phases are studied by nanoindentation. To our knowledge this is the first time that the mechanical properties of this amorphous/nanocrystalline matrix are studied. ICP (In-situ Coating Property) sensor, developed for quality control and residual stress evaluation, is also used to measure the elastic modulus and coefficient of thermal expansion (CTE) of the coatings. Abrasion wear resistance of the coatings are studied according to standard ASTM G 65D.

Because of the brittle nature of HVOF coatings, the main focus of this study is in the effects of coating microstructure on fracture toughness, and on crack initiation and propagation resistance. It is shown that even when two similar coatings have equal indentation fracture toughness values, the critical crack initiation loads may be very different. This new parameter is expected to be extremely useful in the evaluation of the coating performance under loading conditions.

INTRODUCTION

Thermal sprayed cemented carbides such as WC-CoCr coatings are well known and widely used for different wear protection purposes. However, the incomplete understanding of the formation mechanisms and the effects of spraying parameters can often lead to inferior performance of the coatings. The problems associated with increased wear rate, cracking and limited coating thickness arise from the phase changes during deposition, formation of excess residual stresses, porosity, etc. Among different thermal spray methods high velocity oxy fuel (HVOF) spraying has proven to be especially suitable for deposition of carbide coatings because of relatively low flame temperature and supersonic particle velocities [1]. For WC-Co material it is well known that during flight sprayed particles melt to different extents depending on their size, density and dwell times. Molten Co dissolves the WC grains whereas carbon loss occurs by

diffusion through the liquid followed by reaction with the oxygen from the surroundings. There can be large amounts of carbon and tungsten dissolved in the matrix metal, especially in the outer regions of sprayed particles. During cooling, Co-rich liquid becomes supersaturated resulting from the formation of W_2C and other mixed carbides. High cooling rates are responsible of amorphous/nanocrystalline matrix phase. During cooling, precipitation of mixed carbides like *eta*-carbide [$(Co_6W_6)C$] phase may occur in the Co-rich material. All of these effects are most visible on the outer core of the particles. In the small size particles, the whole particle can be affected by decarburization [2]. However, the effect of matrix crystallinity and chromium in the matrix of WC-CoCr is not well understood. Also the mechanical properties of amorphous matrix, which can determine the overall performance of the coating, are completely unknown.

EXPERIMENTAL PROCEDURES

Materials

Agglomerated and sintered WC-10%Co-4%Cr powder from Sulzer Metco WOKA GmbH, Germany, having particle size distribution of 15-45 µm was used. Coatings were deposited by DJ Hybrid 2600 HVOF gun using hydrogen as a fuel gas onto carbon steel, austenitic stainless steel and aluminium substrates. The in-flight particle temperature and velocity was measured during spraying with Spray Watch 2i, (Oseir Oy, Finland). ICP –sensor (In-situ Coating Property) was used to monitor the bending and temperature of the 220 x25 x2.5 mm substrates during spraying.

Microstructural characterization

Morphology of used powder and microstructures of coatings were studied by scanning electron microscopes (FE-SEM, Hitachi S-4700 and JEOL JSM-6400). The particle size distribution of powder was determined by laser diffractometer. The phases of the powder and coatings were characterized by X-ray diffraction (Philips PW3710 with Mo K-alpha radiation and Philips PW3830 with Cu K-alpha) and transmission electron microscope (TEM Tecnai F20 G2 200kV, analysis: EDX and EELS), XRF (LECO) was used to measure oxygen and carbon contents. Porosities of the coatings were determined by applying image analysis of the SEM BSE images with 500x magnification from 3 different cross-sectional locations (Leica QWin Standard v 3.2.1). For the TEM studies the cross sectional coating samples were applied. They were ground to such a small thickness that in the same sample one could place a stack consisting of two similar coating samples and two silicon wafers glued together and inside a 3 mm copper tube. This tube sample was cut into 100 µm discs that were thinned further and then dimple ground from both sides down to 20 µm and finally ion milled from both sides simultaneously with an 3-5 kV Ar beams in order to obtain the hole in the middle of the specimen, e.g. to obtain thin enough region to the coating cross sections for the TEM.

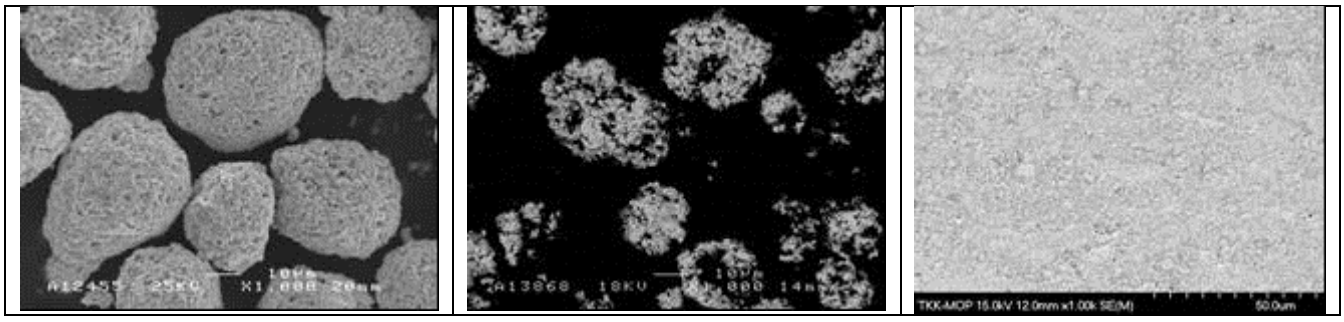

Figure 1. Morphology of the WC-CoCr powder (a) particles and (b) their cross-sections. (c) Cross sectional structure of the WC2 coating. SEM studies carried out in the SE image mode.

MECHANICAL PROPERTIES

Micro hardness and Young´s modulus

Two different hardness methods were used to study the cross-sections and surfaces of the coatings: the conventional Vickers method with optical study of the indentation mark, according to standard EN ISO 14923 and the nanoindentation hardness that was evaluated from the load–displacement data. Elastic- or Young´s modulus was calculated following the procedure proposed by Oliver and Pharr [3].

Fracture toughness

The toughness of a material describes its ability to absorb energy before and during fracture. Because of the brittle nature of most thermal sprayed coatings, fracture mechanics play an important role in evaluation of the usability and performance of the coatings. Fracture mechanical theories, equations and measuring techniques of bulk ceramics, also possessing brittle nature, have been the starting point for studying the fracture behaviour in the thermal sprayed coatings.

Because of the required sample size in other methods, the indentation fracture toughness (IF) method seems to be the only reasonable and suitable one for thermal sprayed coatings. The basic idea in it is to apply large enough load with Vickers diamond tip to initiate cracks from the diagonal corners of the indentation mark. From the average crack length and applied indentation load the fracture toughness (K_{IC}) can be calculated. Fracture toughness K_{IC} describes the critical stress intensity factor of mode I crack.

Indentation fracture toughness K_{IC} can be measured from the cross-section or the surface of thermal sprayed coating. When measured from the surface, one usually gets four corner cracks with the same length and the boundary conditions described in JIS R 1607-1990 can be used. Because of higher loads needed to initiate corner cracks compared to hardness measurements, the maximum plastic depth of the indentation can not be more than one tenth of coating thickness to avoid any substrate effects. Fracture toughness measured from the cross-section of the coating describes the lamella cohesion. The cracks prefer to grow in the direction parallel to the substrate and vertical cracks are rarely produced in HVOF WC-CoCr coatings. The cracks parallel to the substrate will usually initiate and propagate in the lamella boundary as shown in Figure 3. Because of this preferred crack growth direction, the equations and boundary conditions developed for homogenous bulk ceramics cannot apply. If the cracks grow only in parallel direction, the average crack length (l) is calculated by dividing the total

crack length (=sum of the cracks) by two, not by four as when measured from the surface. One requirement is that the cracks should initiate near the diagonal corners. If other major cracks than the corner cracks are developed, the measurement is not valid. This prerequisite may lead to difficulties of finding valid measurements, especially if the coating possesses large residual stresses. The crack can grow with two different ways, depending on the material and applied load. These crack –systems are so called Palmqvist –cracks, which are parabolic surface cracks and so called half-penny –cracks, which are half circle shaped cracks underneath the indentation. It is important to recognize which one of these crack systems is developed because they may require different K_{IC} – equations. In tougher coatings like WC-Co and YSZ the preferred crack geometry is Palmqvist, but in alumina and cromia it is usually half-penny. It also depends on the applied load. The crack geometry identification can be performed by polishing the indented surface. If the cracks stay in contact with the indentation mark after polishing, geometry is half-penny. If gap is developed between indentation mark and cracks, the geometry is Palmqvist.

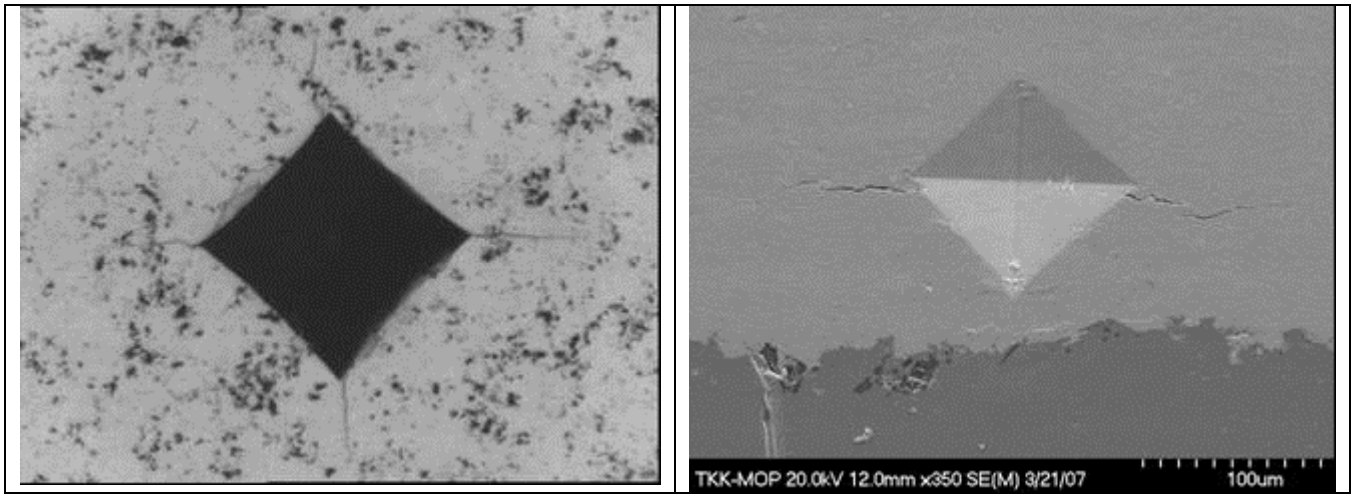

Figure 2. a) Optical image of K_{IC} indentation from the coating surface, b) SEM image from the cross-section, showing only parallel cracks.

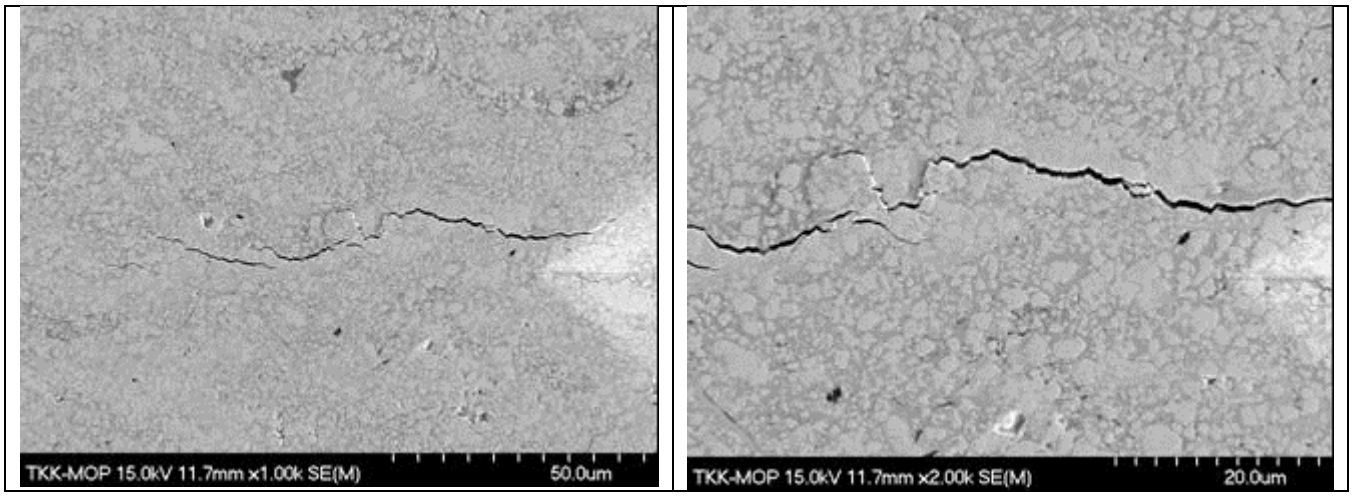

Figure 3. a) Crack does not always initiate from the exact corner of diagonal, because it prefers to initiate and propagate in the overheated lamella boundary, in this WC-CoCr coating. b) Higher magnification of the same SEM –picture.

There are about twenty different indentation fracture toughness formulas developed for bulk ceramics in literature, but all of the equations are based on the same principle: crack length vs. applied load. The most common form of indentation fracture toughness equation is (1) [4], but they are usually valid only for half-penny crack geometry.

$$K_{IC} = \xi\left(\frac{E}{H}\right)^{1/2}\left(\frac{P}{c^{3/2}}\right) \quad (1)$$

where ξ is a material-independent constant for Vickers-produced radial cracks, E is Young's modulus, H is hardness, P applied load (mN) and c is the crack length measured from the centre of indentation (µm). Due to the numerous possibilities, when presenting the indentation fracture toughness values it is crucial to inform what equation was used. In present work, the K_{IC} values are calculated with the Evans – Wilshaw –equation (2) [5], because of preferred Palmqvist crack geometry developed in WC-CoCr coatings.

$$K_{IC} = 0.079\left(\frac{P}{a^{3/2}}\right)\log\left(\frac{4.5a}{c}\right) \quad (2)$$

where K_{IC} = fracture toughness (MPa*m$^{1/2}$), a = indentation half-diagonal (µm), c and P as above. The equation is valid in the range of $0.6 \leq c/a \leq 4.5$. Furthermore it does not use materials hardness or Young´s modulus values, like most K_{IC} –equations do. This eliminates the uncertainty from the hardness (H) and Young´s modulus (E) measurements.

Critical Crack Initiation Load and Crack Propagation Resistance

Two new fracture parameters, the Critical Crack Initiation Load (P_{cr}) and the Crack Propagation Resistance (R_{pr}) of the thermal sprayed coatings, were developed during the study. Both are complementary values for fracture toughness, but they give more valuable information about the usability and life expectancy of coating. The basic principle of the P_{cr} parameter is to evaluate how much load the surface of the coating can withstand without cracking. Especially in the applications and components where crack-free surface is preferred this parameter can

play a significant role when choosing the suitable coating, for example, for wear and/or corrosion protection. Also under fatigue or cyclic loading conditions a higher value of critical crack initiation load can be one of the most important parameters of the coating.

The Critical Crack Initiation Load can be detected from the loading part of the load-indentation depth curve as a jump where load does not increase, but indentation depth seems to advance (Figure 4). This load value correlates to the moment, where the major corner cracks are initiated. As shown in the results section, two similar coatings may have almost the same fracture toughness, but their P_{cr} values can be very different.

In some coatings the critical crack initiation load, P_{cr} is not as visible in the loading curve as above. Here, one can apply a mathematical approach: the coating failure starts when second derivative of the loading curve changes from positive to negative, but the actual critical crack initiation load can be calculated from curve´s third derivative zero position. It points the place where the change in slope is the greatest. The place is demonstrated in figure 5.

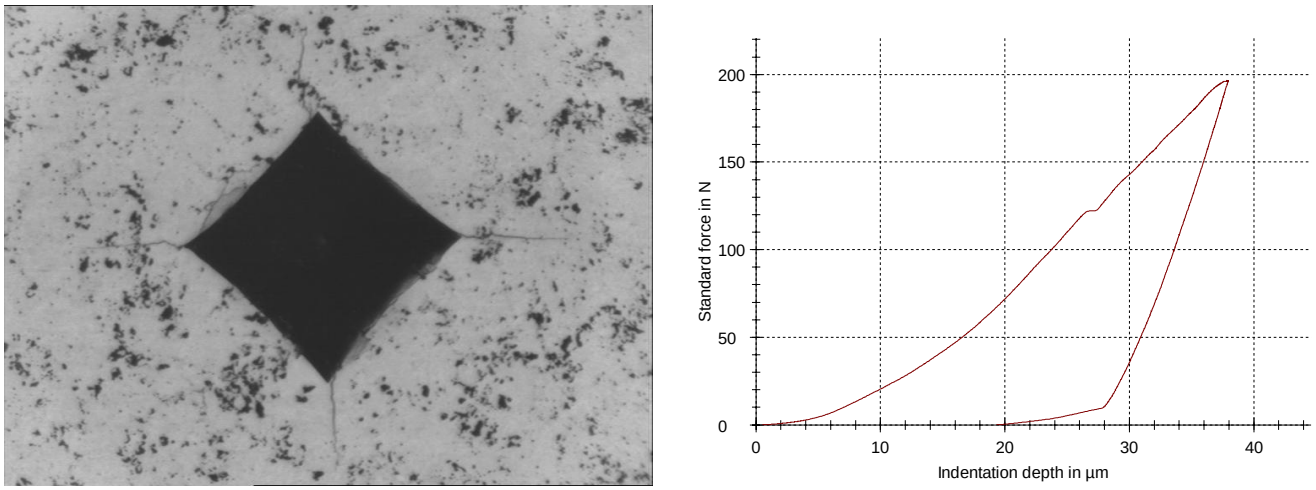

Figure 4. a) Optical image of WC-CoCr surface indented with a 196.2 N (=20 kg) load, b) Load – depth curve of the same indentation. Notice the jump in approximately 125 N in the loading curve, corresponding to the Critical Crack Initiation Load.

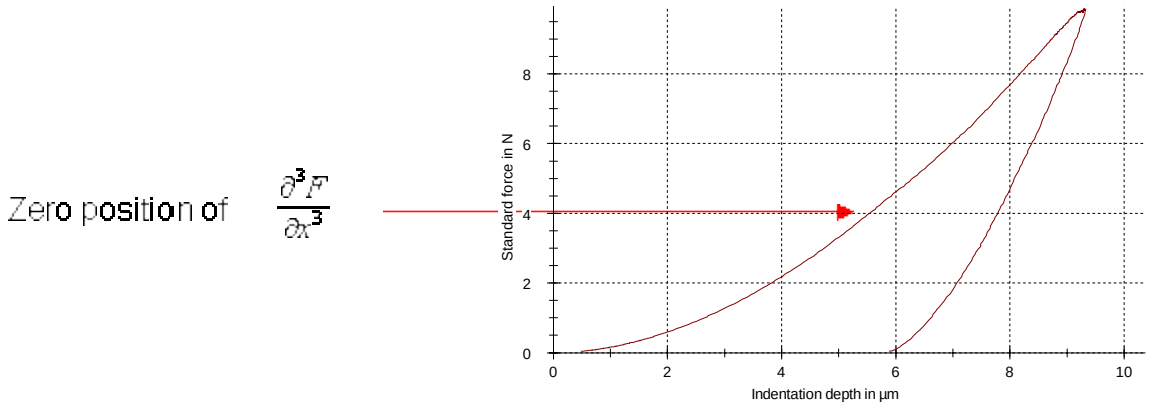

Figure 5. Indentation load vs. depth –curve of yttria stabilized zirconia (YSZ) coating. The zero position of loading curves third derivative is pointed by arrow.

The P_{cr} can be confirmed by indenting the sample with load that is lower than the Critical Crack Initiation Load and checking if any visible corner cracks are formed.

When the Critical Crack Initiation Load is established**,** the Crack Propagation Resistance (R_{pr}) can be determined comparing the slope of the curve before and after the P_{cr}. Loading ranges for slope calculations must be decided based on expected conditions of application. In thermal sprayed coatings factors like intra- and interlamellar porosity can have a major effect on R_{pr}.

Nanoindentation

Nanoindentation (Hysitron Triboindenter) was used for more detailed mechanical property characterization, e.g. for measuring hardness and elastic modulus of carbides and the matrix material of the coating. Even though the dissolution of WC to the matrix is well known the properties of the matrix are not well understood and the values are not available in literature. This is the first time to our knowledge that the mechanical properties of this amorphous (amorphous structure confirmed by TEM studies) matrix is studied.

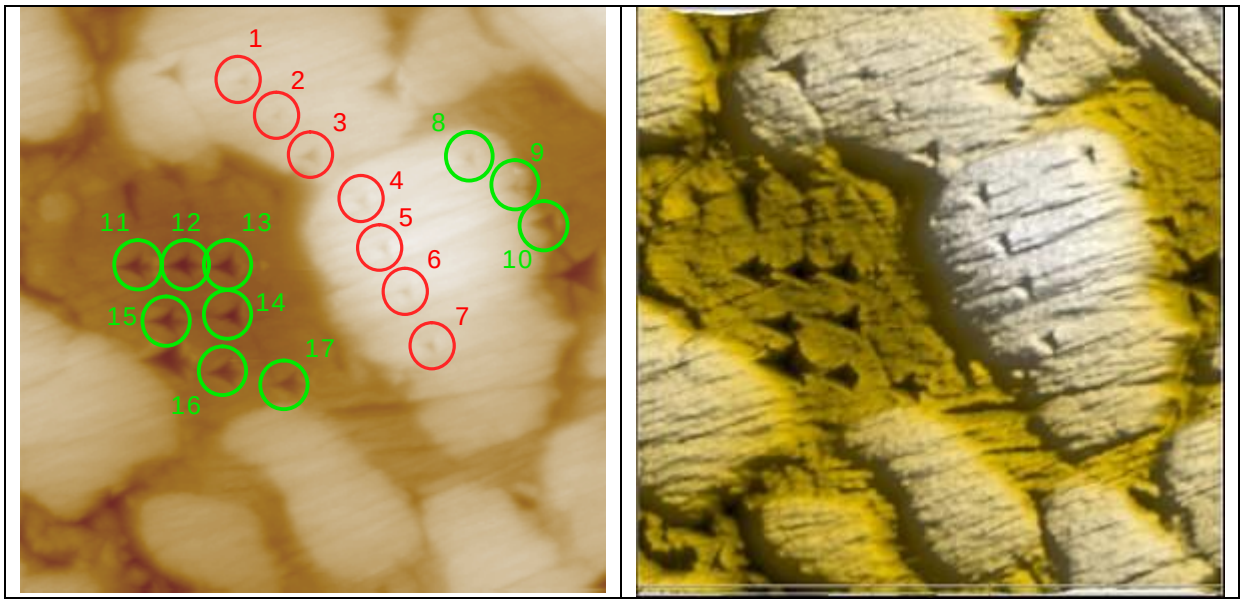

Figure 6. Nanoindentation of WC –particles (red circles, indentations 1-7), CoCr –matrix (green circles, indentations 11-17) and boundary area between them (green circles, indentations 8-10). On the left side the SPM picture and on the right side the AFM picture of the studied area (2 x 2 µm^2).

Wear tests

Two different wear tests were performed. Rubber wheel sand abrasion tests were done according to ASTM G65 D –standard, where samples were placed against rubber wheel with standard surface roughness at a static normal force of 45 N. Round-shaped quartz particles, average size of 250 µm and mass flow of 235 g/min were used. The sliding velocity was 1.86 m/s and test time was 30 minutes for all samples.

Solid particle erosion test was a 90° spray jet of 800 µm average diameter corundum particles. The spray distance was 52 mm, air pressure 4 bars and total of 1200 g of corundum was sprayed in 36 s.

ICP –sensor

In-situ Coating Property (ICP) sensor is a in-situ curvature method, in which the curvature of a thin plate sample is on-line monitored by three lasers during the deposition process. By this way, the various stages of stress build-up can be monitored and the various stress contributions can be evaluated separately. The ICP sensor was used to extract in-plane elastic modulus of the coatings deposited. The curvature sensor is based on laser sensing of deflections in a strip during thermal spraying which is converted to sample curvature. A simultaneous measurement of temperature is achieved via multiple thermocouples. Elastic modulus of the coatings could be calculated from the coating-substrate composite curvature change due to thermal mismatch [6]. Sprayed beams were subjected to low temperature thermal cycling after deposition. In two experiments per sample, a flame torch was used to heat up the composite uniformly up to 150˚C and 250˚C. Later, samples cooled down to room temperature by free convection and cooling portion was taken for analysis. According to the Tsui and Clyne's [7] curvature change model: during cooling, the elastic modulus can be calculated from:

$$\Delta k = \frac{1}{\Delta R} = \frac{6E'_D E'_S t_D t_S (t_D + t_S)\Delta T \Delta\alpha}{E'^2_D t_D^4 + 4E'_D E'_S t_D^3 t_S + 6E'_D E'_S t_D^2 t_S^2 + 4E'_D E'_S t_D t_S^3 + E'^2_S t_S^4} \quad (3)$$

where Δk is the curvature change due to the decrease in temperature (ΔT) and $\Delta\alpha$ is the difference in the coefficients of thermal expansion (CTEs) between deposit and substrate. t_D is the deposit thickness, t_S is the substrate thickness, and E'_D and E'_S are the moduli of deposit and substrate respectively.

Continuous monitoring of curvature and temperature during heating-cooling experiment allowed estimation of the deposit modulus by curve fitting method. By spraying similar coatings with similar parameters on substrates having different CTEs, the CTE of the coating can be determined by iterating the unknowns E_C and α_C.

MICROSRUCTURE OF THE COATINGS

The main idea of the present study was to increase the understanding of the effect of structure and phases of HVOF WC-CoCr coatings on their mechanical behaviour. Knowledge of the effects of these factors was increased by applying several new investigation methods.

Overall very dense coating structures were produced by applying varying deposition conditions. Appreciable differences in the densities are observed in the cross-sectional microstructures of the various coatings with different F/O-ratios (= Fuel gas flow divided by oxygen gas flow) and positions in the T-v –chart (average in-flight particle temperature-velocity chart, Figure 8). Obtained results point out the importance of particle melting state in the density of the coatings. Most dense coatings were produced by using F/O – ratios 2.2 and 2.5, with which the melting of the particles is sufficient. In general, coatings made with parameters producing lower particle temperatures and lower total gas flows showed higher porosity. Coating porosity seems to correlate strongly on the mechanical properties and the high values can be only obtained when critical density for the coating is reached.

TEM studies were made to further understand the properties of coatings and the structural state of the matrix. One of the studied coatings was WC 2 (Table 1.). According to the EDX- analysis the matrix contains Co, Cr and W. EDX can not detect carbon because of

its light atomic weight, but it was confirmed with EELS measurements that there was also carbon in the matrix. In Figure 7a and c the amorphous nature of the matrix is confirmed, actually, in the studied samples there was no crystalline structure in the matrix at all. It has been shown before that in WC-Co HVOF coatings the Co –matrix can be mostly nanocrystalline[2]. It is assumed that presence of Cr in the matrix alloy promotes the formation of amorphous phase compared to pure cobalt matrix. In Figure 7a, a metallic tungsten precipitate is shown surrounded by amorphous matrix.

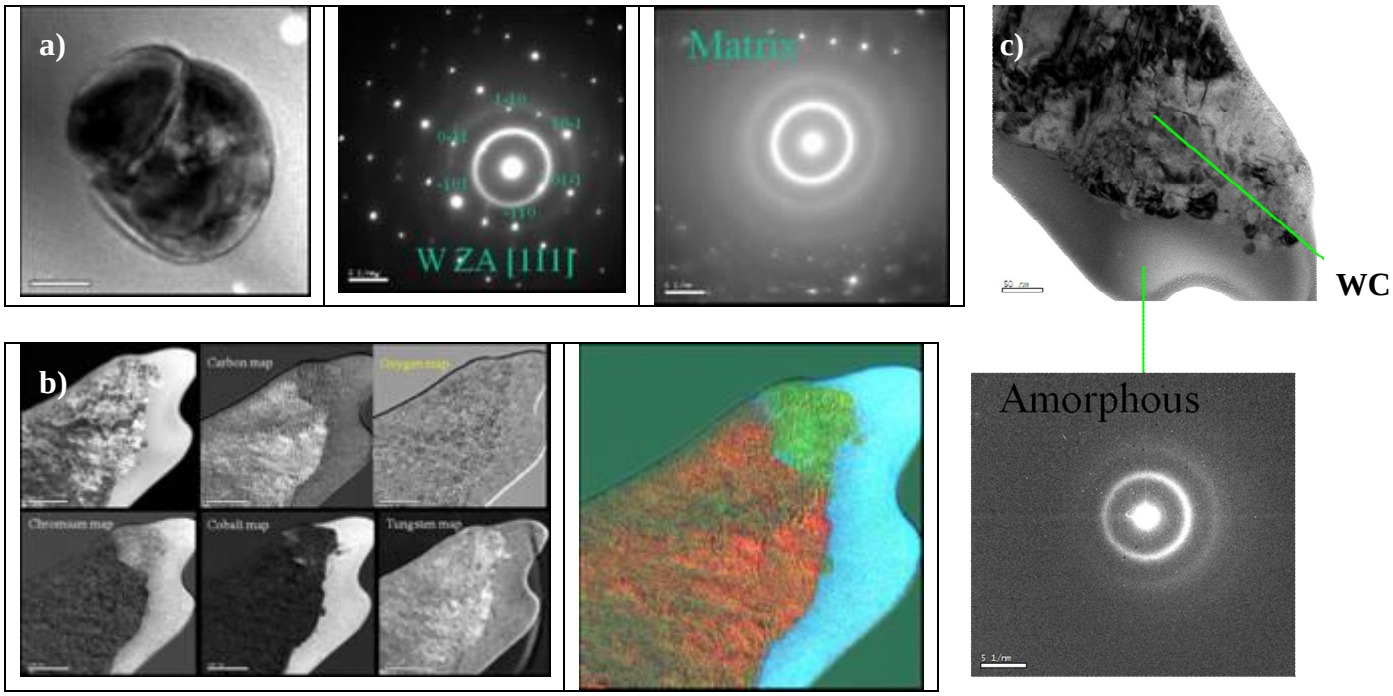

Figure 7. a) Metallic tungsten precipitate surrounded by amorphous matrix and their SAD (selected area diffraction) patterns respectively. Scale in the left side picture is 50 nm, b) Elemental 30ev EFTEM images. Scale in the left side pictures is 100 nm. Red colour indicates carbon, green chromium and blue cobalt in the right hand picture, c) TEM images showing the amorphous matrix and crystalline WC full of dislocation networks.

RESULTS AND DISCUSSION

Interesting relations between the F/O-ratio and, for example, the in-flight particle temperature were detected during spraying of WC-CoCr when using the Spray Watch 2i. It can be seen from Figure 8. that in-flight particle temperature can be adjusted by F/O-ratio if the back pressure is kept constant. This requires adjustments in the total gas flow rate. If the total gas flow is kept constant, the change in F/O-ratio will also change the back pressure value. Thus, the velocity of the sprayed particles can be controlled by regulating the chamber pressure and particle temperature can be adjusted by changing the F/O-ratio. This gives a possibility to move in the T-v space horizontally and vertically.

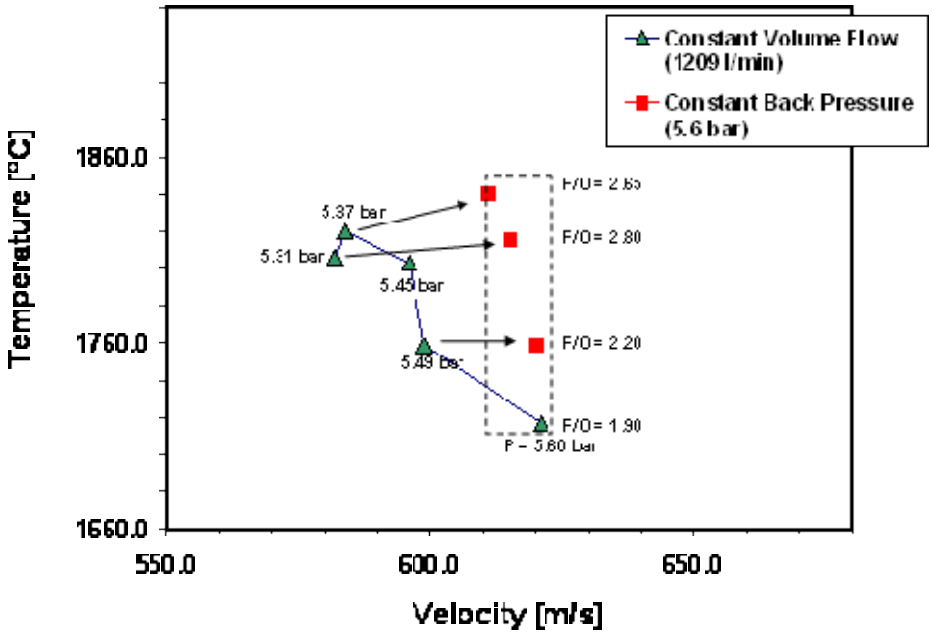

Figure 8. In-flight particle diagnostics describing the effects of spraying parameters.

Table 1. Properties and parameters for constant volume flow (1209 l/min) coatings. cs=cross-section, s=surface.

Sample	F/O-ratio	H_{cs} [Hv 0.3]	H_s [Hv 0.3]	Abrasive Wear [mg/30min]	$E_{curvature}$ [GPa]	E_{cs} [GPa]	E_s [GPa]	$K_{IC,cs}$ [MPam$^{1/2}$]	$K_{IC,s}$ [MPam$^{1/2}$]
WC 1	1.9	1306	1235	13.0	294	301	253	5.45	7.37
WC 2	2.2	1518	1404	9.2	376	376	297	6.14	6.69
WC 3	2.5	1597	1510	10.0	346	341	287	5.72	5.41
WC 4	2.8	1448	1526	10.3	321	321	309	5.70	7.10
Sample	P_{cr} [N]	Carbon content [wt-%]	Oxygen content [wt-%]	W_2C/WC	Chamber pressure [bar]	Volume flow [l/min]	Average particle T [°C]	Average particle v [m/s]	Porosity [%]
WC 1	210	5.3	0.36	0.16	5.6	1209	1828	594	0.42
WC 2	125	5.0	0.27	0.22	5.49	1209	1864	585	0.01
WC 3	164	4.7	0.23	0.31	5.45	1209	1876	574	0.23
WC 4	220	5.0	0.21	0.28	5.31	1209	1860	558	0.19

Coatings with exactly the same spraying parameters, except with lower total volume flow of 1184 (l/min) were also produced. Abrasive wear rates increased from 6% to 35%, cross-sectional hardness and fracture toughness decreased from 14% to 23% and from 19% to 27% respectively, curvature elastic modulus decreased from 10% to 26% and porosity was between 0.22% and 0.57%, depending on F/O-ratios. Higher total volume flows were also used to achieve constant back pressure 5.6 bars with different F/O-ratios as shown in Figure 8. Comparison between 5.49 bars and 5.6 bars, both with 2.2 F/O-ratio is shown in Table 2.

Table 2. Comparison of coatings sprayed with F/O-ratio 2.2, but with different chamber pressures.

Sample	F/O-ratio	Chamber pressure [bar]	Volume flow [l/min]	W_2C/WC	P_{cr} [N]	$K_{IC,s}$ [MPam$^{1/2}$]	$E_{curvature}$ [GPa]	E_{cs} [GPa]
WC 2	2.2	5.49	1209	0.22	125	6.69	376	376
WC 5	2.2	5.6	1253	0.15	162	7.41	396	353
Sample	E_s [GPa]	Abrasive wear [mg/30min]	H_{cs} [Hv 0.3]	H_s [Hv 0.3]	Average particle T [°C]	Average particle v [m/s]	Porosity [%]	Particle erosion [mg/36s]
WC 2	297	9.2	1518	1404	1864	585	0.01	26.2
WC 5	360	10.6	1604	1399	1759	620	0.17	28.1

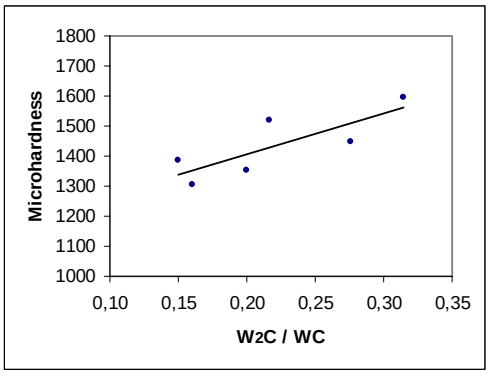

a)

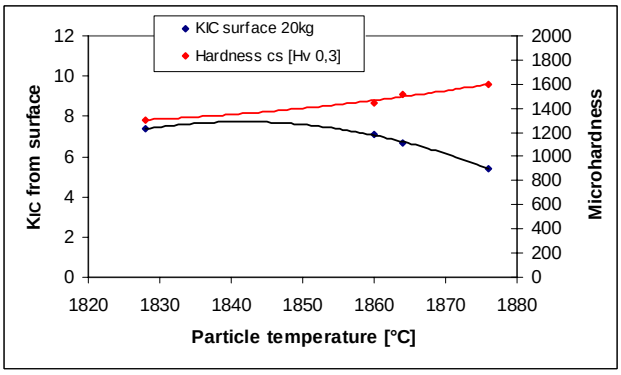

b)

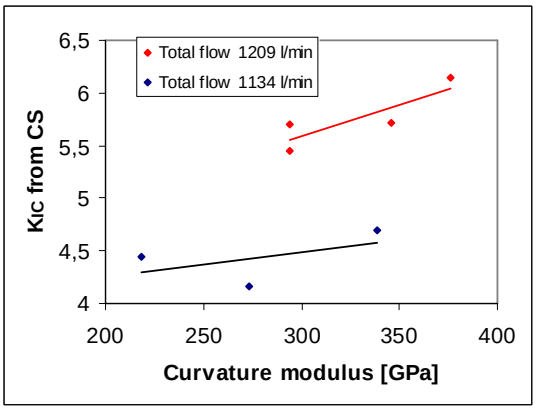

c)

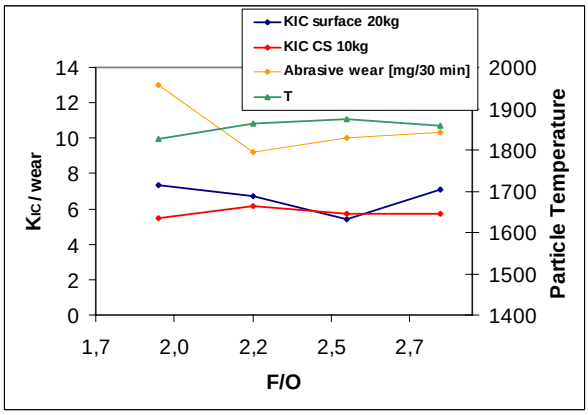

d)

Figure 9. Some correlations between process parameters and the properties of the coatings (cs=cross-section).

Higher total volume flow resulted higher chamber pressure, higher average particle velocity and lower average particle temperature. The dissolution of carbides was lower (W_2C/WC –ratio) and this can be observed as higher surface fracture toughness and Critical Crack Initiation Load.

In Figure 9 is presented correlations between process parameters and the properties of the coatings. According to Figure 9a the hardness of the WC-CoCr coating increases when the amount of the W_2C content is increased, e.g. when carbon loss and its solubility to matrix has been higher. It is clear from Figure 9a and

b that the formation of W_2C is linked to the heat input for the particle during spraying process. Here, the matrix is strengthened and the ductility of the matrix phase is decreased at the same time. Therefore, the increase of coating hardness is rather resulting from hardening of the matrix, and not directly from the W_2C formation. Higher solubility of C and W to the CoCr –matrix helps the matrix to solidify amorphous. Amorphous metallic phases are known to be harder, but also more brittle, than the crystallized phase of the same material. This was confirmed here with the cobalt-chromium matrix by nanoindentation technique while its amorphous state was verified with the TEM studies. It should also be noticed that when the temperature of the spray particles increases, the hardness of the coating increases, while the fracture toughness measured from the coating surface decreases. Furthermore, a significant difference between K_{IC} measured from the surface and from the cross section can be found. As the surface K_{IC} value is related to the particle heat load, the cross-section K_{IC} is related to the composition of lamella boundaries, lamella cohesion and interlamellar porosity. Cross-sectional cracks are initiated and propagated at the lamella boundaries as shown in Figure 3. This behaviour is also revealed in Figure 9d in the "cold" ends of the temperature curve. The top surface K_{IC} has its highest value with the coldest process parameters, when the carbide solubility is the lowest. The cross-sectional K_{IC} is at maximum at the F/O-ratio 2.2. This same F/O-ratio ensures also the best wear resistance, as the abrasion wear and solid particle erosion wear are at minimum. When the total volume flow decreases, the porosity of the coating increases and its K_{IC} drops. It can be concluded that there is a correlation between the elastic modulus and fracture toughness measured from the cross section of the coating, and these values are connected to the properties of the lamella interfaces. However, K_{IC} values measured from the top surface describes more inherent state of the lamella. In abrasive wear there seems to be some advantage from the hardening of the matrix phase. The case can be different, for example, if load carrying capability is needed, then the more dominant parameter is the surface K_{IC} and the Critical Crack Initiation Load P_{cr}.

WC-CoCr samples WC 1 and WC 2 which were sprayed with the same spraying parameters and conditions, except F/O–ratio was 1.9 for WC 1 and 2.2 for WC 2. In WC 2 sample both the elastic modulus and hardness from the cross-section and from the surface are higher. W_2C / WC ratio is also higher for sample WC 2. Thus, the higher heat load during spraying has lead to strengthened matrix which is seen in higher stiffness (elastic modulus) and higher hardness.

Fracture toughness measured from the cross-section is also higher for the coating WC 2. This was expected, because the higher melting stage of particles gives better wetting, meaning better lamellar cohesion and lower interlamellar porosity. However, this result should not be miss-interpreted so that the coating WC 2 is more ductile than WC 1 as the cross-sectional fracture toughness is primarily connected to the cohesion of lamellas. Actually, the ductility of WC1 matrix is more preserved during spraying, and this can be seen in higher top surface fracture toughness value. K_{IC} value measured from the surface describes more inherent state of the lamella. The most surprising thing is the huge difference in the Critical Crack Initiation Load (P_{cr}), which is almost two times higher for sample WC 1. Examples of critical crack initiation load measurements are shown in Figure 10.

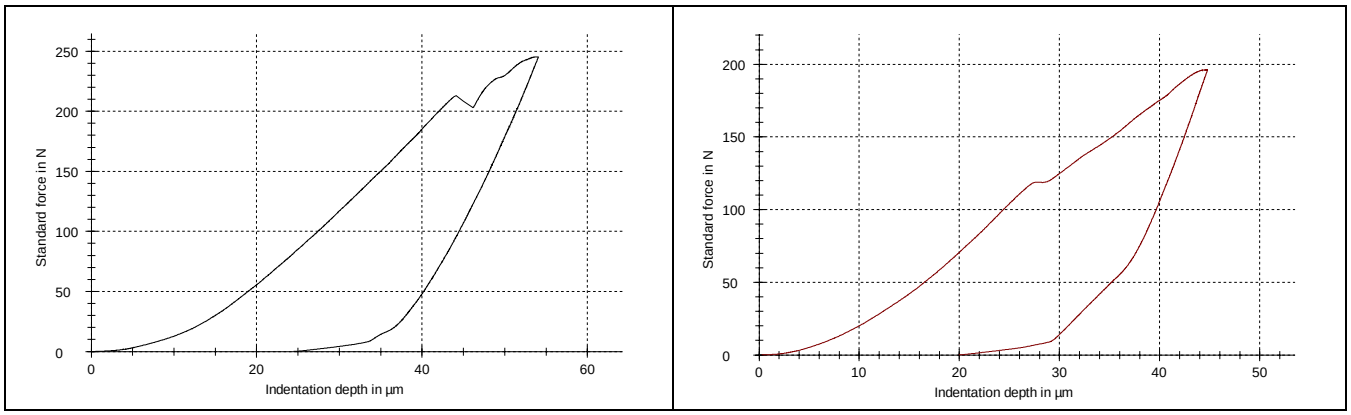

Figure 10. Load-depth –curves of samples the coatings WC1 and WC2. The step connected to the critical crack initiation load is (a) in WC 1 at 210 N, and (b) in WC 2 at 125 N.

The repeatability of these measurements was confirmed for WC-CoCr -coatings. All of the measurements of sample WC 1 showed P_{cr} to be between 203–220 Newtons, when the range was 115–130 Newtons for sample WC 2. These results were further confirmed by indenting the sample surfaces with loads lower than the critical crack initiation loads and no visible corner cracks were formed.

The mechanical properties of coating matrix and WC phase were measured using instrumented nanoindentation. The adhesion between matrix and carbides was examined by nanoindentations in the boundary areas. The elastic modulus and hardness values of the matrix and WC phases are shown in Table 3. for WC 2 sample. A careful study of the indent marks by SPM (scanning probe microscopy) imaging provides further information in understanding the performance of coatings.

Measured elastic modulus of WC is very close to the theoretical value. The hardness of the matrix phase is relatively high reaching the average value of 17.5 GPa. Therefore, it can be concluded that the performance of the coating can be linked to the mechanical state of its microstructure that is a highly strengthened during spraying. Excellent wetting and adhesion between matrix and carbides were confirmed by indenting the phase boundaries (example in Figure 6. indentations no. 8-10). No cracks or separation of phases were found. Indentations were performed in different locations and with different loads (400, 800 and 2000 µN). The measurements were repeatable, no differences were found between used loads or measuring direction (cross-sectional or surface sample) and standard deviations were low. The values of the matrix were relatively high and it might be caused by work hardened layer which was formed during the cutting and polishing of the sample. Even really thin work hardened layer would cause problems, because of shallow indentation depths. A suitable etching agent should be found and used to verify the results.

Table 3. The average indentation results from the matrix and the carbides of WC2 sample.

Phase	E [GPa]	H [GPa]	$E_{literature}$ [GPa]
WC	625 ± 33	33.8 ± 2.7	669 – 696
CoCr	365 ± 18	17.5 ± 0.8	211 – 248 (crystal.)

ICP sensor was used for determination of the elastic modulus and CTEs (coefficient of thermal expansion) of the coatings as well as for studying the stress build-up during coating deposition. The results in Table 4 shows that with the ICP sensor, modulus values are comparable to the indentation modulus values from the cross-sections. The most critical factor for the modulus measurement when applying the ICP sensor equipment, is the correct CTE value. The determination of CTE was carried out applying the method described above (Eq.3). After deposition the CTE is possible to iterate from the data collected during deposition of the same coating on different substrates. Theoretical CTE value of WC-10%Co4%Cr is $6.13x10^{-6}$ K^{-1}, but because of such factors as phase changes and decarburization, it was expected to change during spraying. With the help of three different substrate materials, the iterated CTE values were $5.3x10^{-6}$ K^{-1} for F/O-ratios 1.9, 2.5 and 2.7 and $5.1\text{-}5.2x10^{-6}$ K^{-1} for F/O-ratio 2.2.

Table 4. Comparison of modulus values measured with different methods (Curvature modulus is measured with ICP-sensor, cs=cross-section, top=surface).

Curvature modulus [GPa]	Indentation Modulus CS [GPa]	Indentation Modulus Top [GPa]
301	301	253
319	321	309
376	376	297
342	341	287

Based on the data achieved in the study, the predicted contours of the values can be presented by using MODDE D-optimal analysis. An example is presented in Figure 11.

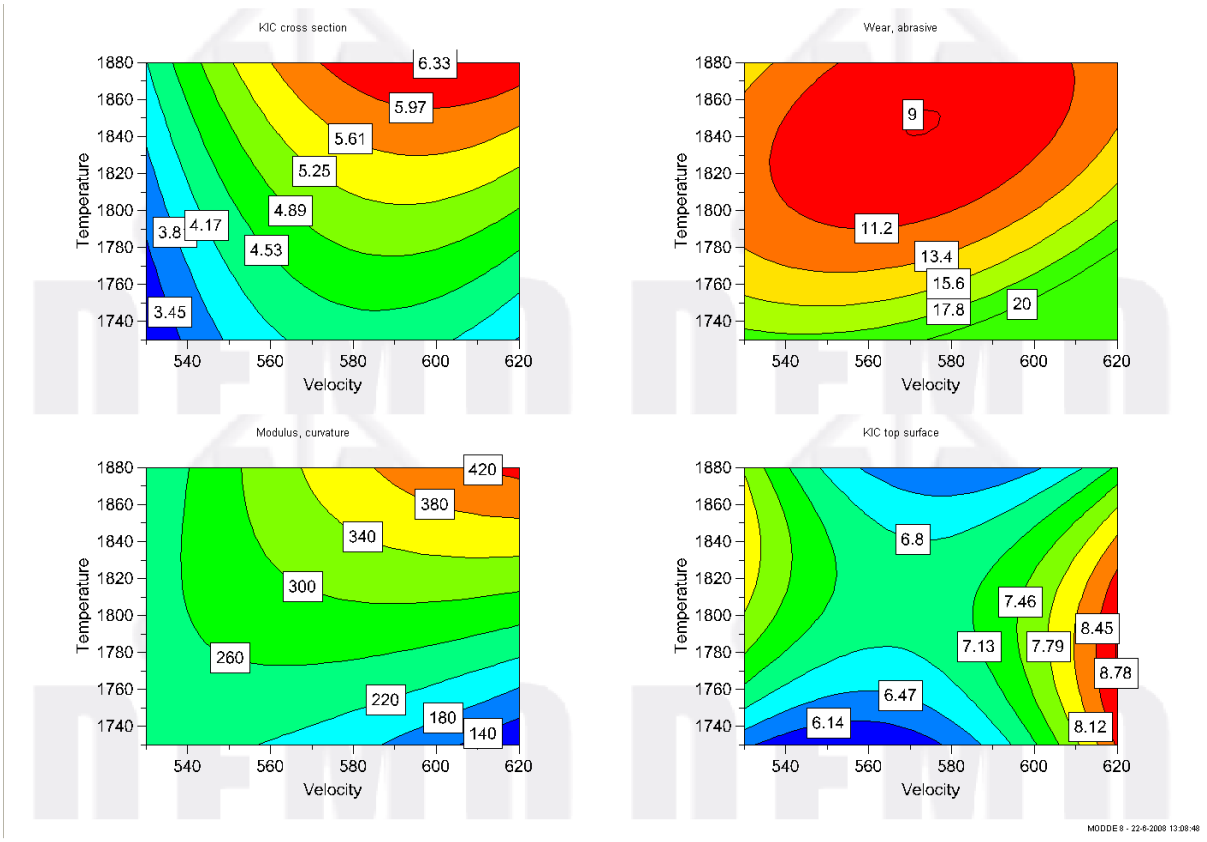

Figure 11. Example of process Maps for WC-CoCr coatings based on the results of this study.

CONCLUSIONS

Some generalised conclusions can be derived from the results obtained. The maximum abrasive wear resistance can be achieved when the particle melting is high enough to produce dense inherent lamella structure. This realizes at the F/O-ratio 2.2. At the same location in T-v-plot the fracture toughness measured from the cross-section and curvature modulus reached highest value. Like earlier discussed this is due to hardening of matrix phase and good lamella cohesion. However the fracture toughness and Critical Crack Initiation Load measured from the surface is maximum at lower temperatures, which leads to the conclusion that the fracture properties inside lamella can be measured from the surface. These values can be important in different type of wear conditions.

REFERENCES

J.R.Davis (Ed.), Handbook of Thermal Spray Technology, 2004, ASM International.

C.Verdon et al., A Study of High Velocity Oxy-Fuel Thermally Sprayed Tungsten Carbide Based Coatings. Part 1: Microstructures, Mat.Sci.and Eng. A246 (1998) p.11-24.

W.C.Oliver and G.M.Pharr, An Improved Technique for Determining Hardness and Elastic-Modulus Using Load and Displacement Sensing Indentation Experiments, Jour.of Mat.Res. 7 (1992) 6, p.1564-1583.

G.R.Anstis et al., A Critical Evaluation of Indentation Techniques for Measuring Fracture Toughness: I, Direct Crack Measurements, J.Am.Cram.Soc., 64 (1981) 9, p.533-538.

Evans A.G., Wilshaw T.R. Quasi-static solid particle damage in brittle solid. I. Observations analysis and implications, Acta Metall. 24 (1976). 939-956.

J.Matejicek and S.Sampath, In-situ Measurements of Residual Stresses and Elastic Moduli in Thermal Sprayed Coatings: Part 1: Apparatus and Analysis, Acta Materialia, 51 (2003) 3, p.863-872.

Y.C.Tsui and T.W.Clyne, An analytical model for predicting residual stresses in progressively deposited coatings, Part 1: Planar geometry, Thin Solid Films, 306 (1997) 1, p.23-33.